Physical properties from VLT spectroscopy of a sample of star-forming dwarf galaxies at intermediate redshift[1]

Lucía Rodríguez-Muñoz[1], Jesús Gallego[1], Pablo G. Pérez-González[1], Laurence Tresse[2], Armando Gil de Paz[1], Guillermo Barro[3], Víctor Villar[1], and Olivier Le Fèvre[2]

[1] Departamento de CC. de la Tierra y Astrofísica II, Facultad de CC. Físicas, Universidad Complutense de Madrid
[2] Aix Marseille Université, CNRS, LAM (Laboratoire d'Astrophysique de Marseille) UMR 7326, 13388, Marseille, France
[3] University of California, Santa Cruz

Abstract

Dwarf galaxies remain as one of the most important and missing pieces of the great puzzle of formation and evolution of galaxies. Due to their low luminosities, their study has been mainly biased to the local universe or clusters, which hampers our knowledge of their redshift of formation and properties along the cosmological time, strong observational tests to recent models of formation and evolution of low-mass galaxies. Using the multiwavelength database RAINBOW, that provides photometric redshifts and masses estimations, we selected a representative sample of dwarf galaxies in the Chandra Deep Field-South (CDFS) within the redshift range $0.3 < z < 1$. We present the results of the spectroscopic study of our sample, carried out using own spectra obtained with the spectrograph VIMOS at the VLT-ESO. These observational data provide spectroscopic redshifts and measurements of emission lines such as [OII]3727Å , Hβ, [OIII]4958,5007Å , and Hα, from which we estimate the physical properties of our dwarf galaxy sample.

1 Introduction

Dwarf galaxies play a key role in galaxy formation and evolution. Among other reasons: 1) hierarchical models predict that low-mass systems merged to form massive galaxies (building

---

[1]Based on observations made with ESO Telescopes at the La Silla Paranal Observatory under programme 088.A-0321

block paradigm, e.g. [4]); 2) dwarf systems might have been responsible for the reionization of the Universe (e.g. [18]). While the history of low-mass dark matter halos is relatively well understood, the formation history and evolution of dwarf galaxies is still poorly reproduced by the models due to the distinct evolution of baryonic and dark matter. Observations of the scatter of the ionization fraction of cosmic hydrogen indicate that star formation in low-mass dark matter halos with masses below $10^{10}\,\mathrm{M_\odot}$ should have been quenched after the end of reionization ($z \sim 6$) due to the high temperature reached by the intergalactic medium (IGM, e.g. [18]). The epoch when the IGM cooled down enough to allow these very low-mass galaxies form stars again is uncertain. Theoretical models disagree about the density of low-mass systems at different redshifts, in particular, recent models predict two main formation redshifts for galaxies that depend on the mass (e.g. [12]), while Local Group dwarfs seem to have been forming stars uninterruptedly since at least $z \sim 1 - 2$ (e.g. [7]).

   The observational study of dwarf galaxies, has been traditionally carried out in clusters and the local universe, due to their intrinsically low luminosity. However, in both cases the cosmological information is generally blurred, and even lost, due to the fact that: 1) interactions with close neighbours dominate the evolution of galaxies within high density environments, and 2) the little evolution in the photometric properties of stellar populations with ages $\geq 10\,\mathrm{Gyr}$ limits the determination of precise redshifts of formation.

   To deepen our knowledge about the impact of the temperature of the IGM on the formation of dwarf galaxies, and their evolution along cosmic time, we need to determine accurate star formation histories, as a good approach to their formation redshift, and study their physical properties at different and intermediate redshifts so that they have stellar populations still sensitive to age changes. Thus, we decided to perform a spectroscopic study of a sample of low-mass star-forming field galaxies at intermediate redshift. In Section 2 we describe how we select them. Section 3 details the spectroscopic survey carried out using VIMOS at VLT, and finally, in Section 4 we present some of the properties found. We adopt a concordance cosmology: $H_0 = 70$ km s^{-1} Mpc^{-1}, $\Omega_\mathrm{M} = 0.3$, $\Omega_\Lambda = 0.7$.

2   The sample

The sample of low-mass star-forming galaxies was built on a SUBARU NB816 [13] image of the CDFS field, using the RAINBOW database [14, 3], that provides estimations of photometric redshifts, spectral energy distributions, and stellar masses, based on multi-wavelength ancillary data from UV to far-IR. We also used the morphology catalogs developed by Griffith et al. (now updated in [8]) on GOODS-S and GEMS fields. We considered two different criteria: 1) stellar mass $< 10^8\,\mathrm{M_\odot}$, and 2) the classic definition of Blue Compact Dwarf (BCD) galaxies: $M_{B,0} > -18$ (AB) mag, $(B-V)_0 < 0.6$ and $S_{R_\mathrm{eff},B,0} < 23$ mag arcsec^{-2} [17]. An extra criterium was considered taking into account the sensitivity of VIMOS: $m_\mathrm{SUBARU\,NB816,AB} < 26$ mag. Among dwarfs, BCDs present observational advantages such as strong emission lines, as a result of the star-formation burst they undergo, and high surface brightness, that make them good tracers of low-mass objects at intermediate redshifts. Furthermore, BCDs present an underlying stellar component, testimony of their early star formation history. The redshift range considered was $0.3 < z < 1$, and this criterium was applied to the photometric redshifts.

Table 1: Observations details

Pointing	RA [J2000]	Dec [J2000]	Date	Exposure t. [s]	Slits
1	03h 32m 33.5s	$-27° \; 45' \; 26.3''$	17-Nov-2011	12000	119
2	03h 32m 22.8s	$-27° \; 51' \; 09.5''$	18-Nov-2011	9600	119

The limit at $z = 0.3$ is given by the lowest z for which the lookback time is still long enough (~ 3 Gyr) to provide some improvement in the age estimations. Moreover, SDSS dwarfs at $z < 0.25$ are studied in detail [2]. We found 675 galaxies with stellar mass $< 10^8 \, M_\odot$ and 816 BCDs covering an area of ~ 441 arcmin^2.

3 Observational data

The spectroscopic observations were carried out with VIMOS [11] at VLT in visitor mode. We chose medium resolution grism MR as a compromise between resolution ($R \sim 580$) and wide wavelength range $\lambda\lambda 4800$Å $- 10000$Å , well suited to cover from [OII]3727Å to Hα for the lowest redshift dwarfs of interest ($z \sim 0.3 - 0.5$), and from [OII]3727Å to [OIII]5007Å for the highest redshift of the sample ($z \sim 1$). Observations were planned as two 4 hours pointings (6×2400 s), each of them on a slightly different area of CDFS, to observe 238 targets (192 dwarfs with and $M_* < 10^8 \, M_\odot$ and 46 BCDs), covering a total of 414 arcmin^2. Unfortunately, instrument operational problems brought as a result some setbacks that prevented the fulfilment of the program. Details of the observations finally performed can be found in Table 1. Observing conditions were photometric and seeing mean value was ~ 0.6 arcsec for both nights. Finally, an standard star was also observed to perform absolute flux calibration.

The reduction process of the data was performed using the VIMOS Interactive Pipeline Graphical Interface (VIPGI, [16]). A total of 79 precise redshifts were measured using the EZ tool [6]. For the rest of the cases, either no detection was found or not enough spectral features were identified. The properties (mass, absolute rest-frame magnitudes, etc.) of those objects spectroscopically confirmed were recalculated using software developed by our group. Thus, the final spectroscopic sample can be summarized as: 18 dwarfs ($M_* < 10^8 \, M_\odot$, some of them also BCDs), 22 BCDs (with $M_* > 10^8 \, M_\odot$) and 39 other low-mass objects (90% $M_* < 10^{9.5} \, M_\odot$). It is worth noting the importance of these numbers, given the lack of spectroscopic data for dwarf galaxies in the literature at such redshifts ($0.3 < z < 1$).

4 General properties

In the following sections we show the extreme character of the sample with values of stellar masses that reach $\sim 10^6 \, M_\odot$, and rest-frame B absolute magnitudes close to ~ -12 (AB) mag. We compare the properties of the samples selected with the different criteria. Dwarfs selected by mass meet BCDs rest-frame B absolute magnitude and blue color criteria in all cases but

seem to have lower average surface brightness. On the other hand, the selection based on BCDs properties present a wide range of stellar masses, not reaching as extremely low values as dwarfs, but always below $\sim 10^{9.5}\,\mathrm{M_\odot}$. Samples are morphologically heterogeneous but they can be classified mainly into two types: 1) BCD-like galaxies, characterized by a compact shape and one (or a few) vigorous star-formation node, and 2) dIrr, similar but with eased characteristics and wider range of properties, they normally present a not negligible diffuse region. Such is the case of *tadpole* galaxies, a frequent shape present in our sample. In Fig. 1a we show the HST/ACS images of some of the galaxies in our samples.

4.1 Structural parameters

In order to analyse the nature of the galaxies selected we make use of the scaling relationships between size, mass and luminosity and the differences in their behaviour with respect to representative values of local galaxies (Fig. 3a in [15] and references therein). In Fig. 1b we plot the luminosity against surface brightness, calculated using the effective radius from the morphology catalogs developed by [8]. We can see that BCDs populate the same area as local spheroidals due to their compact morphology. Dwarfs ($< 10^8\,\mathrm{M_\odot}$) spread over a wider range of surface brightness that includes the BCD (or spheroidal) region, but reaching also the area dominated by irregulars and extremely low values of surface brightness $> 25\,\mathrm{mag\,arcsec^{-2}}$.

In Fig. 1c we represent the mass-luminosity relationship for local star forming galaxies from [5]. We can clearly see how our targets follow the same sequence but showing an excess in luminosity for a given mass. This difference is also found in our sample between objects located at redshifts below or above 0.5. We also point out the extreme character of our sample: we extend the relationship to lower masses and higher redshifts than previous studies.

4.2 Excitation

The excitation regime of the ionized gas can be studied through the [OIII]5007Å /Hβ flux rate. In Fig. 1d we represent this value versus $M_{B,0}$ for our targets and a sample of local star-forming galaxies [5]. In this diagram, star-forming galaxies populate a sequence that covers from high excitation and low luminosity values, corresponding to low metallicity objects such as HII galaxies, for which the star formation process dominates the luminosity, to low excitation and high luminosity values, corresponding to more evolved galaxies with well established stellar populations such as disk-like galaxies. Extremely metal poor galaxies appear outside the sequence. Such is the case of IZw18, also represented in the diagram. Our sample follows the overall star-forming sequence in the excitation-luminosity diagram, populating mainly the high excitation regime area.

4.3 Nature of their emission

The so-called BPT diagrams [1] based on the [OIII]5007Å/Hβ and [NII]6583Å/Hα emission line flux rates, help us to identify the nature of the emission of the galaxies of our sample and to constrain the metallicity and excitation scenario. We were able to measure [NII]6583Å
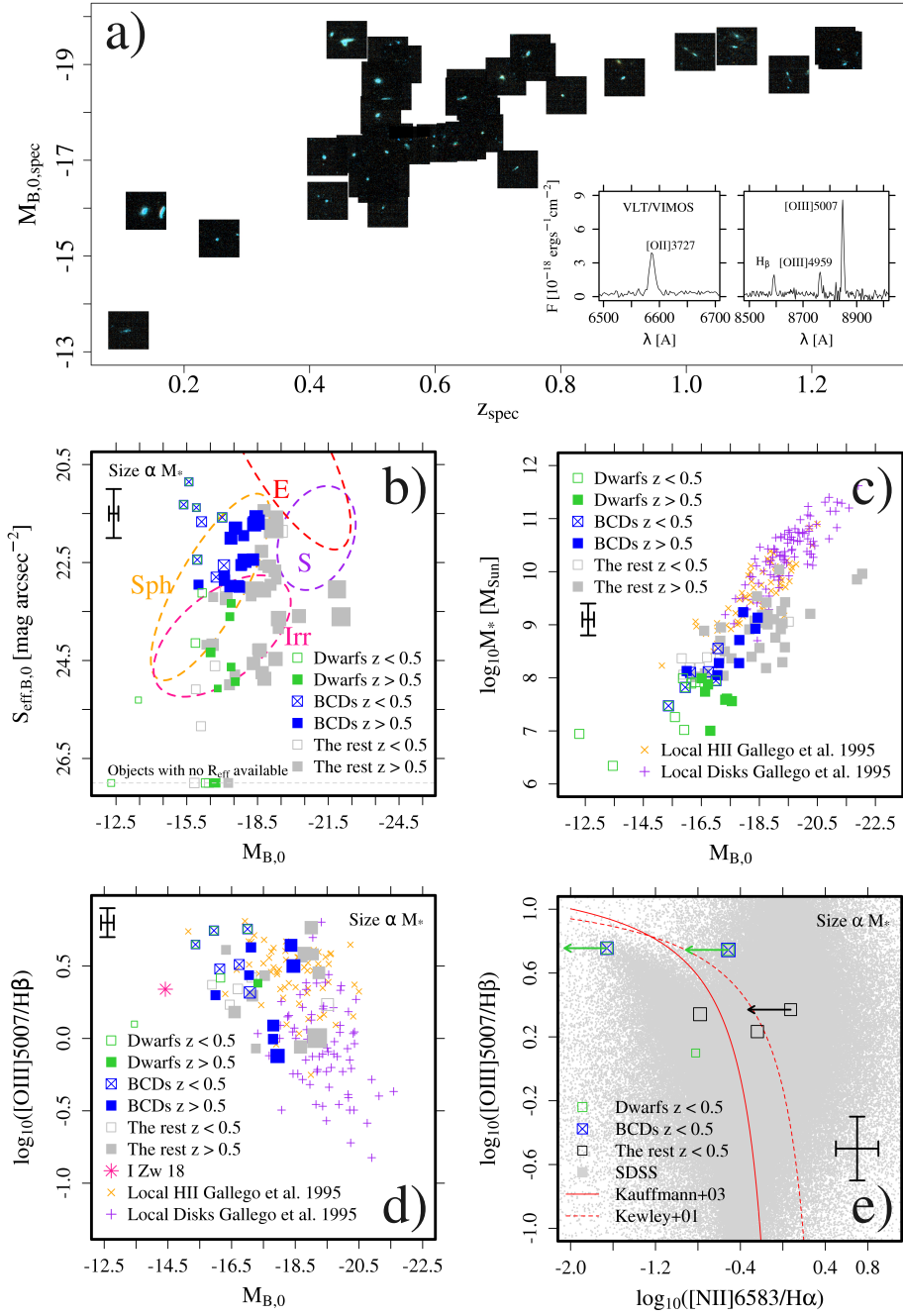
Figure 1:   a) 5×5 arcsec^2 RGB images built using v and z HST/GEMS bands. VIMOS spectrum of a BCD with $M_* < 10^8\,M_\odot$ of our sample. b) Surface brightness and luminosity diagram (see text for details). c) Stellar mass luminosity relationship for star-forming galaxies (see text for details). d) Excitation diagram (see text for details). e) BPT diagram. We overplot SDSS data for comparison. Unclear detections of [NII]6583Å are represented with arrows and considered maximun values for the flux rate. AGN, transition and star formation areas are delimited by the curves defined by [9] and [10].

and Hα fluxes for 6 galaxies, 3 dwarfs (two of them also BCDs) and 3 low-mass objects, and we adopted an optimistic approach to identify the unclear detections. From the results, shown in Fig. 1e, we can assure there is no evidence of AGN contribution. Our targets are located overall in the star-forming region. Furthermore, their location in the upper-left area of the plot indicates that low metallicity and high ionization regime is the most probable for our targets, as expected.

References

[1] Baldwin, J. A., Phillips, M. M., & Terlevich, R. 1981, PASP, 93, 5

[2] Barazza, F. D., Jogee, S., Rix, H-W., et al. 2006, ApJ, 643, 162

[3] Barro, G., Pérez-González, P. G., Gallego, J., et al. 2011, ApJS, 193, 13

[4] Dekel, A. & Silk, J. 1986, ApJ, 303, 39

[5] Gallego, J., Zamorano, J., Aragón-Salamanca, A., & Rego, M. 1995, ApJ, 455, 7

[6] Garilli, B., Fumana, M., Franzetti, P., et al. 2010, PASP, 122, 827

[7] Grebel, E. K., Gallagher, J. S. III, & Harbeck, D. 2003, AJ, 125, 1926

[8] Griffith, R. L., Cooper, M. C., Newman, J. A., et al. 2012, ApJS, 200, 9

[9] Kauffmann, G., Heckman, T. M., Tremonti, C., et al. 2003, MNRAS, 346, 1055

[10] Kewley, L. J., Dopita, M. A., Sutherland, R. S., Heisler, C. A., & Trevena, J. 2001, ApJ, 556, 121

[11] Le Fèvre, O., Vettolani, G., Maccagni, D., et al. 2003, The Messenger 111, 18

[12] Mamon, G. A., Tweed, D., Thuan, T. X., & Cattaneo, A. 2012, in *Dwarf Galaxies: Keys to Galaxy Formation and Evolution*, JENAM 2010 Symposium S3, pp. 39-46

[13] Ouchi M., Mobasher, B., Shimasaku, K., et al. 2009, ApJ, 706, 1136

[14] Pérez-González, P. G., Rieke, G. H., Villar, V., et al. 2008, ApJ, 675, 234

[15] Phillips, A.C., Guzmán, R., Gallego, J., et al. 1997, ApJ, 489, 543

[16] Scodeggio, M., Franzetti, P., Garilli, B., et al. 2005, PASP, 117, 1284

[17] Thuan, T. X, & Martin, G. E. 1981, ApJ, 247, 823

[18] Wyithe, J.S.B. & Loeb, A. 2006, Nature, 441, 322